

Defect mode in the bulk plasmon-polariton gap for giant enhancement of second harmonic generation

F. Reyes Gómez,¹ J. R. Mejía-Salazar,^{2,*} Osvaldo N. Oliveira Jr.,² and N. Porrás-Montenegro¹

¹*Departamento de Física, Universidad del Valle, AA 25360, Cali, Colombia*

²*Instituto de Física de São Carlos, Universidade de São Paulo, CP 369, 13560-970, São Carlos, São Paulo, Brasil*

(Received 27 April 2017; revised manuscript received 28 July 2017; published 21 August 2017)

We demonstrate that the defect mode in the bulk plasmon-polariton gap of one-dimensional defective metamaterial photonic crystals can be used to achieve a giant enhancement of more than four orders of magnitude in the second harmonic (SH) conversion efficiency only by changing the incidence angle. Furthermore, the one-dimensional photonic crystal may be designed in order for the SH wave to coincide with the edge of the Bragg gap or with the defect mode inside this gap, in which case the enhancement is even higher. Because of the robustness of the bulk plasmon-polariton gap to scaling effects, the present proposal may inspire different routes for frequency upconversion, signal filtering, and switching photonic devices.

DOI: [10.1103/PhysRevB.96.075429](https://doi.org/10.1103/PhysRevB.96.075429)

I. INTRODUCTION

Existing microstructuring and numerical modeling techniques allow one to design and develop artificial materials, better known as metamaterials, whose permittivity and/or permeability is a function of the incident frequency [1–26]. One of the most remarkable properties of these metamaterials is the possibility of a simultaneous negative value for permittivity and permeability, thus leading to a negative index of refraction. Striking electromagnetic phenomena arise with a negative index, including the reversed Doppler effect predicted by Veselago in the 1960's [27]. In one-dimensional photonic crystals (PCs) comprising periodic alternating layers of positive/negative refractive materials, forbidden frequency ranges appear. These photonic band gaps (PBGs) have physical origins entirely different from conventional Bragg scattering mechanisms [28–31], and are referred to as zero- \bar{n} [28] and plasmon-polariton [29] (PP) non-Bragg gaps, known to be robust against disorder and scale effects [30,31]. The zero- \bar{n} gap is observed due to a zero geometrical averaged refractive index, and can exist for any θ value. The PP gap is due to the coupling of the longitudinal electric/magnetic field component of light with the corresponding plasmonlike effective response of metamaterial layers under transverse magnetic (TM)/transverse electric (TE)-polarized incident light, and therefore can only be observed under obliquely incident light. In the case of materials with only their permittivity (ϵ)/permeability (μ) being frequency dependent, the corresponding bulk PP gap can only be observed for TM/TE-polarized incident light.

Nonlinear inclusions in PCs exhibit features that may be exploited in such technological applications as optical switching, optical buffering, and frequency upconversion for improved near-infrared detection [32–34]. Solitons have been excited in a negative index Fabry-Pérot étalon [34], in a cavity filled with a negative refractive material [35], and gap-soliton modes [36] were observed at the gap edges of zero- \bar{n} [37] and bulk PP [38] gaps. Large enhancement factors for second harmonic generation (SHG) were obtained around the

zero- \bar{n} and the bulk PP gaps in one-dimensional metamaterial PCs [39–41], which is promising for high-order frequency conversion and short-wavelength laser sources applied in large screen laser displays and photoelectron spectrometers [42–45]. Strongly enhanced SHG in cavities obtained with one-dimensional periodic PCs [44–51] can be achieved by breaking the periodicity, e.g., by incorporation of a defect layer, which leads the system to act as a cavity with distributed mirrors. The corresponding cavity (defect) mode is located inside the PBG, and the electromagnetic field profile is strongly localized within the defective layer, thus enhancing the light-matter interaction. Surface plasmon-polariton (SPP) excitations have been used for SHG [52–55], but there is a lack of interest in the bulk PP. The PP gap has been extensively studied, but the possibility to excite a defect mode in this gap was only recently demonstrated [56]. This defect mode has the peculiarity of being observed only for a nonzero incident angle, $\theta \neq 0$. The corresponding frequency can be controlled by means of the incident angle, which may inspire different routes for switching and filtering applications [57–61].

In this paper, we theoretically demonstrate that the defect mode inside the bulk PP gap, where a strong light-matter coupling is present, can be employed to enhance the efficiency of SHG up to giant values. Our concept employs the control of the light-matter interaction through the dependence on the angle of incidence to enhance the nonlinear effects. This is promising, on one hand, because the high localization of the defect mode, combined with the simultaneous strong light-matter interaction in the bulk PP gap, can reduce the optical power required to activate the SHG process. On the other hand, it can also be used in filters or in frequency multipliers due to the very well-defined frequency of the defect modes.

II. THEORETICAL FRAMEWORK

The system we investigate is a finite one-dimensional multilayer structure made by alternating slabs of nonlinear dielectric LiNbO₃ [42,50], labeled A, with a negative refractive metamaterial, labeled B, incorporating a linear dielectric defect layer of AIAs [62], labeled D. Although the energy dissipation inherent in metallic building blocks of metamaterials becomes a restriction in the optical regime, where collective

*jrmejia3146@gmail.com

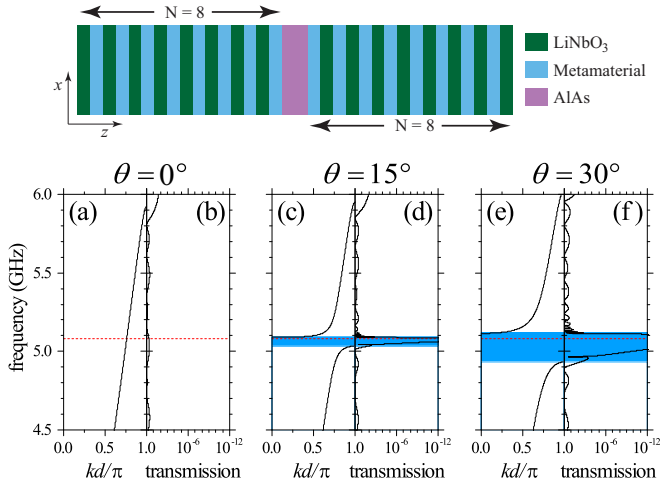


FIG. 1. The upper figure depicts the multilayer architecture under study. (a), (c), and (e) are the photonic band structures for the infinite periodic one-dimensional metamaterial stack for $\theta = 0^\circ$, $\theta = 15^\circ$, and $\theta = 30^\circ$, respectively. The system was considered in the linear regime and losses in metamaterial layers were neglected. k is the corresponding Bloch wave vector along the z direction, $d = a + b$ is the period length, and θ corresponds to the angle of incidence of the TE-polarized light. The highlighted regions represent the plasmon-polariton gap, while the dashed lines indicate the magnetic bulk plasmonlike frequency of metamaterial layers, i.e., the frequency f_p for which $\mu_B(f_p) = 0$. (b), (d), and (f) show the transmission spectra for the finite linear defective one-dimensional metamaterial PC, $(AB)^8D(BA)^8$, for $\theta = 0^\circ$, $\theta = 15^\circ$, and $\theta = 30^\circ$, respectively. For calculation purposes we have taken $a = 10.4$ mm, $b = 5.0$ mm, and $l = 16.0823$ mm, with $\gamma = 0.0001$.

electron oscillations in the metals dictate the metamaterial properties [18], in the microwave and midinfrared frequencies (considered in this work) metals can be approximated as perfect conductors because the skin depth is much smaller than the feature size of the structure. Taking this into account and the available techniques to grow low-loss negative refractive metamaterials from the microwave [17,24,26] to the near- and midinfrared [18,21] regimes, we shall perform the calculations considering no loss or small losses. For simplicity, the multilayer architecture has mirror symmetry around the defect layer, i.e., $(AB)^N D (BA)^N$, for N bilayers AB on each side of the defect, as shown in the upper panel of Fig. 1. LiNbO₃ and ultrathin metamaterial slabs (~ 200 nm) may be produced by lithographic techniques [11,20], and therefore the proposed system should be experimentally feasible with present technologies. For the sake of simplicity we will consider the permittivity and permeability as described by [37]

$$\varepsilon_B = 1.6 + \frac{40}{0.81 - f^2 - if\gamma}, \quad (1)$$

$$\mu_B = 1.0 + \frac{25}{0.814 - f^2 - if\gamma}, \quad (2)$$

with the damping factor $\gamma = 0.0001$. For the linear building blocks, layers B and D, we take the second-order nonlinear susceptibility $\chi^{(2)} = 0$, while for nonlinear LiNbO₃, layers A, we use $\chi_A^{(2)} = 6.7$ pm/V in the microwave regime [63,64].

The incident electric field amplitude $E_0 = 10^7$ V/m (intensity ~ 13.3 MW/cm²) was used to compare with previous theoretical proposals [40]. The layer thicknesses were taken as $a = 10.4$ mm, $b = 5.0$ mm, and $l = 16.0823$ mm, for layers A, B and D, respectively. Refractive indices for LiNbO₃ (AlAs), related to the fundamental frequency (FF) and SH waves, were $n_A^{(1)} = 2.157$ ($n_D^{(1)} = 2.902$) and $n_A^{(2)} = 2.237$ ($n_D^{(2)} = 3.015$), respectively, according to Refs. [47,62]. We consider here the case of a TE-polarized incident wave. If the backcoupling of power from the SH to the FF is neglected, i.e., in the nondepleted pump approximation, the corresponding electromagnetic fields are obtained by solving the following set of coupled equations [40,62],

$$\left[\frac{d^2}{dz^2} + (k_{iz}^{(1)})^2 \right] E_i^{(1)} = 0, \quad (3)$$

$$\left[\frac{d^2}{dz^2} + (k_{iz}^{(2)})^2 \right] E_i^{(2)} = -(k_{0z}^{(2)})^2 \chi_i^{(2)} (E_i^{(1)})^2, \quad (4)$$

where $\chi_i^{(2)}$ is the second-order nonlinear susceptibility in the i th layer. $k_{iz}^{(j)} = n_i^{(j)} k_0^{(j)} \cos(\theta_i^{(j)})$, $k_0^{(j)} = \frac{j\omega^{(j)}}{c}$, $k_{0z}^{(j)} = k_0^{(j)} \cos(\theta_0^{(j)})$, and $\theta_i^{(j)}$ denote the corresponding wave vectors and propagation angles for the FF ($j = 1$) and SH ($j = 2$) waves. The transfer matrix method (TMM) has been used to study SHG in nonlinear one-dimensional PCs under normal incident electromagnetic fields, but it was only recently extended to consider dielectric one-dimensional PCs under oblique incident light [62]. Equations (3) and (4) for oblique incident light were solved with the TMM in Ref. [62], by imposing the initial conditions $E_0^{(2)+} = 0$ and $E_i^{(2)-} = 0$, with $E_0^{(2)+}$ and $E_i^{(2)-}$ being the corresponding forward and backward SH waves at the media before and after the one-dimensional PC, respectively; initial values for the SH are null since there is no incident SH wave. Conversion efficiencies for the forward and backward SH waves are calculated as $\eta_f = \frac{|E_f^{(2)+}|^2}{|E_0^{(1)}|^2}$ and $\eta_b = \frac{|E_b^{(2)-}|^2}{|E_0^{(1)}|^2}$ [50], respectively, while the total conversion efficiency is calculated as $\eta = \eta_f + \eta_b$ [39].

III. RESULTS AND DISCUSSION

The photonic band structures (PBSs) for a perfect infinite periodic one-dimensional PC, built by alternating layers A and B, for TE-polarized incident light are shown in Fig. 1, for incident angles $\theta = 0^\circ$, $\theta = 15^\circ$, and $\theta = 30^\circ$. PBSs were calculated by solving the linear problem imposing the well-known Bloch-Floquet periodic boundary conditions [65]. For comparison, we also plot the corresponding transmission spectra for a finite $(AB)^8D(BA)^8$ defective one-dimensional PC. The dashed line indicates the magnetic bulk-plasmon frequency f_p , i.e., the frequency for which $\mu_B(f_p) = 0$. In TE polarization, the electric field \mathbf{E} is normal to the plane of polarization, the xz plane, while the magnetic field $\mathbf{H} = \mathbf{H}_{TE,\parallel} + \mathbf{H}_{TE,\perp}$ is found along that plane, with $\mathbf{H}_{TE,\parallel} = |\mathbf{H}| \cos \theta \hat{\mathbf{x}}$ and $\mathbf{H}_{TE,\perp} = |\mathbf{H}| \sin \theta \hat{\mathbf{z}}$, where $\hat{\mathbf{x}} = (1, 0, 0)$ and $\hat{\mathbf{z}} = (0, 0, 1)$, indicating the components parallel and normal to the interfaces. For $\theta \neq 0$ there is a photonic band gap, which broadens around f_p with increasing θ . Such a gap is highlighted in the PBSs and transmission spectra in Fig. 1 for

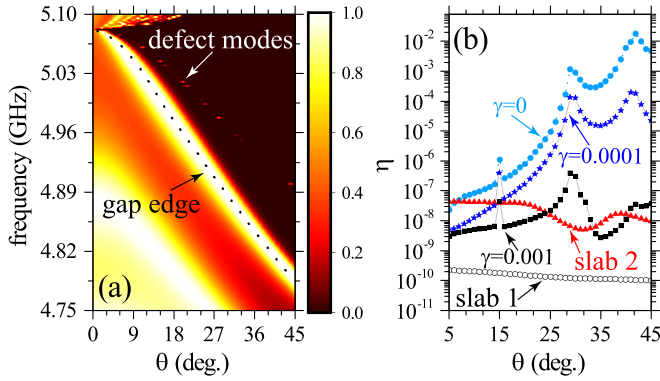


FIG. 2. (a) Transmission spectra around the lower PP gap edge as a function of the frequency and θ . The dotted line is just to guide the eye along the lower PP gap edge. (b) Conversion efficiency for SHG as a function of θ for the FF in the defect mode inside the PP gap.

$\theta = 15^\circ$, and $\theta = 30^\circ$. This PP gap [29] is due to the coupling of the longitudinal magnetic field component of light, $\mathbf{H}_{\text{TE},\perp}$, with the plasmonlike $\mu(f)$ effective response of metamaterial layers. Also observed in Fig. 1 are very sharp transmission peaks inside the PP gap, which correspond to the excitation of the corresponding defect mode. Our interest here is in the nonlinear properties of this defect mode, which is found near the low edge [see Fig. 2(a)]. The rationale is to take advantage of the localized electromagnetic field in defect modes and the strong light-matter interaction in the bulk PP gap to enhance the SH conversion efficiency.

Figure 2(a) displays the transmittance as a function of the frequency and the angle of incidence θ with the bulk PP gap broadening with increasing θ , as expected because $\mathbf{H}_{\text{TE},\perp}$ increases with θ . The dotted line in Fig. 2(a) is a guide for the eye for the bulk PP gap edge. High transmission peaks above the PP gap edge show the corresponding defect mode inside the PP gap as a function of frequency and θ . Figure 2(b) shows the calculated SH conversion efficiency η for the defect mode in the PP gap as a function of the incident angle from $\theta = 5^\circ$ up to $\theta = 45^\circ$. Further increases of θ are accompanied by a wider PP gap that makes it hard to numerically obtain the corresponding defect mode for larger θ values. Calculations were made for three hypothetical values of γ , viz., 0, 0.0001, and 0.001, in order to show the detrimental role of absorption in the SHG process. For larger absorption values the defect mode and nonlinear effects are hindered. For comparison purposes, the SH conversion efficiency is also plotted as a function of θ in the cases of an isolated slab of LiNbO₃ with thickness $a = 10.4$ mm, named slab1, and a slab of LiNbO₃ with the thickness of the total system $L = 228.4823$ mm, named slab2. A slight decrease is observed as θ increases for these slabs, in contrast with the case of the defective PC. It is seen that η can be enhanced by increasing the light-matter coupling (increasing $\mathbf{H}_{\text{TE},\perp}$) with θ . The larger η value for $\theta = 15^\circ$ occurs because the geometrical parameters have been selected to have simultaneous FF and SH waves being defect modes at this θ . This enhancement is therefore due to the excitation of dual-localized defect modes [47], as confirmed in Figs. 3(a) and 3(b). There is a giant value of η for $\theta = 30^\circ$, ascribed to the combination of the high density of states and a slowing

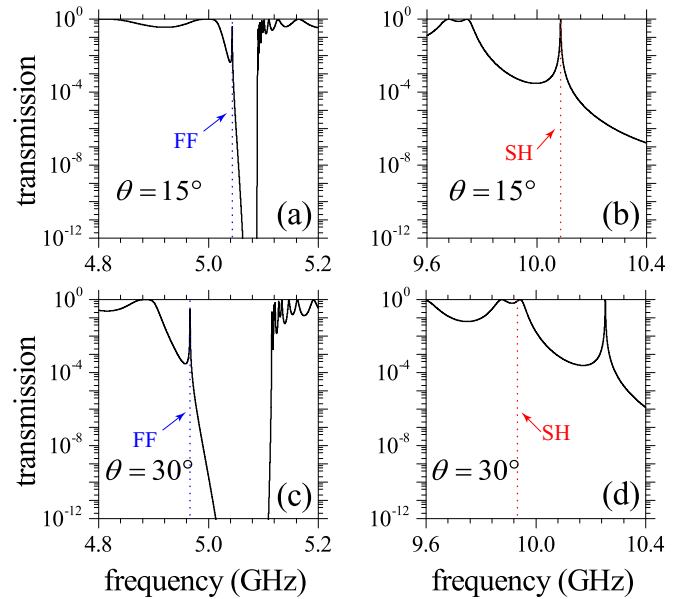


FIG. 3. (a) and (c) are the transmission spectra for TE-polarized incident light, obliquely impinging on the PC with $\theta = 15^\circ$ and $\theta = 30^\circ$, around the corresponding FF. (b) and (d) are the nonlinear transmission spectra for the TE-polarized SH wave, excited by fields in (a) and (c), respectively.

down of the optical waves near the PBG edge [50]. Indeed, Figs. 3(c) and 3(d) show that FF remains as the defect mode in the PP gap, while the SH wave corresponds to a Bragg gap edge for $\theta = 30^\circ$. The enhancement of η for $\theta = 30^\circ$ is larger than for $\theta = 15^\circ$ because the SH conversion efficiency depends not only on the incident field but also on the enhancement of the FF and SH waves in the PC. The corresponding field profiles normalized to the incident fields for the FF and SH

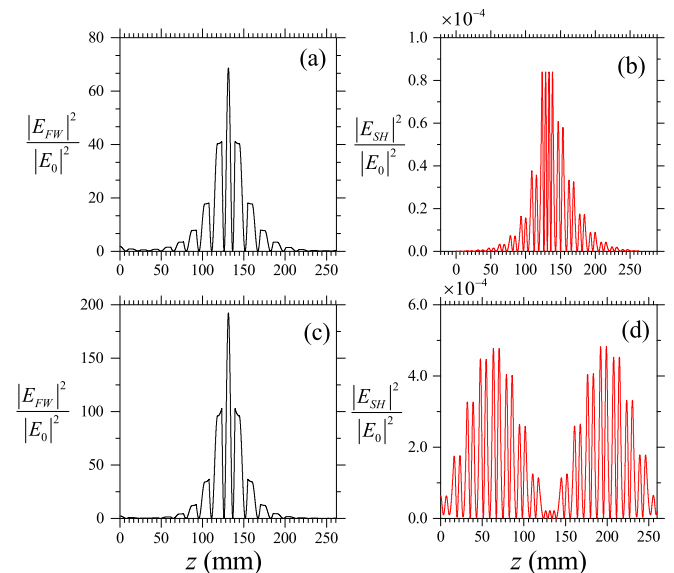


FIG. 4. (a), (b) Field profiles showing dual localization for the FF and SH waves in Figs. 3(a) and 3(b), when both are defect modes. (c) and (d) are the field profiles when FF is the defect mode in the PP gap and the SH wave is found along a Bragg gap edge, as in Figs. 3(c) and 3(d).

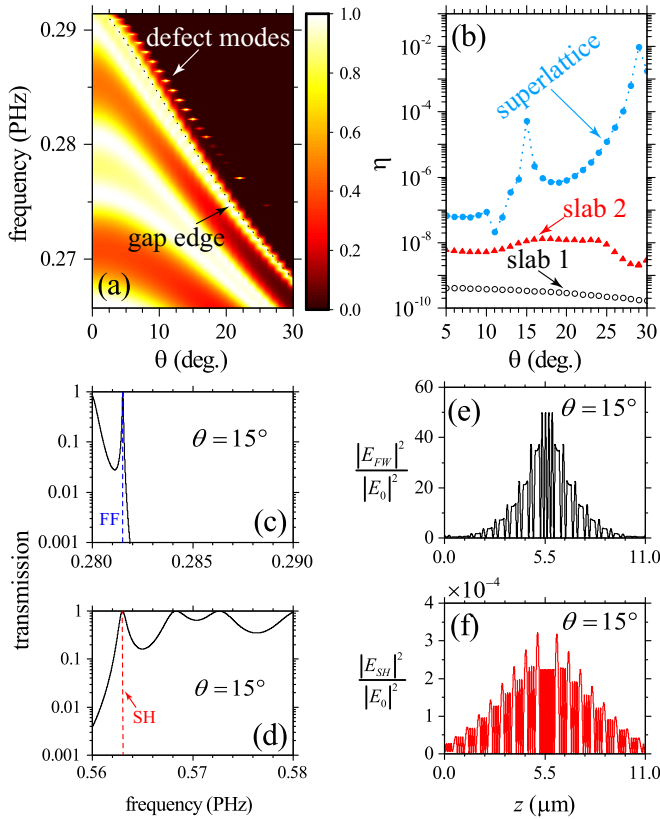


FIG. 5. (a) Transmission spectra around the lower PP gap edge as a function of the frequency and θ . The dotted line is just to guide the eye along the lower PP gap edge. (b) Conversion efficiency for SHG as a function of θ for the FF in the defect mode inside the PP gap. (c) and (d) are the transmission spectra for TE-polarized FF and the corresponding SH wave, for light obliquely impinging on the PC with $\theta = 15^\circ$. (e) and (f) are the field profiles when FF is the defect mode in the PP gap and the SH wave is found along a Bragg gap edge, as in (c) and (d).

waves are shown in Fig. 4, where the amplitude of the SH field for $\theta = 15^\circ$ is approximately 1/5 the value for $\theta = 30^\circ$. One should note that the results above were obtained in the microwave regime, where double negative metamaterials are widely known [13].

In order to extend these results to cases of experimentally feasible one-dimensional metamaterial PCs working at terahertz frequencies, we consider low-loss metamaterials with a negative index of refraction working from the near-infrared to the visible regime [9–12,14,19]. We take the nonlinear susceptibility for LiNbO₃ layers as $\chi_A^{(2)} = 40$ pm/V, according to Refs. [63,64] in the terahertz regime. Layer thicknesses will be considered as $a = 424.4$ nm (LiNbO₃), $b = 225$ nm

(metamaterial layers), $d = 860$ nm (AIAs defective layer), arranged as depicted in Fig. 1. The corresponding results are shown in Fig. 5, where, for simplicity, metamaterial layers were also considered as made by combining the split-ring resonators (SRRs) into a periodic medium such that there is strong coupling between the resonators. The effective permeability and permittivity are thus [1,2]

$$\mu = 1 - \frac{F\omega^2}{\omega^2 - \omega_0^2 + i\omega\gamma}, \quad (5)$$

$$\varepsilon = \varepsilon_\infty + \frac{\tilde{\omega}}{\omega_0^2 - \omega^2 - i\omega\gamma}, \quad (6)$$

where the parameters $\tilde{\omega} = \omega_0\sqrt{\varepsilon_\infty - \varepsilon_0}$, $\omega_0 = \frac{2\pi c}{1550 \text{ nm}}$, $\varepsilon_0 = 3.0$, $\varepsilon_\infty = 1.5$, $\gamma = 3.4 \times 10^{-6}$ PHz, and $F = 0.55$, are determined by the geometrical and material properties of SRRs [1]. c corresponds to the light velocity in vacuum. The optical source is a neodymium-doped yttrium aluminum garnet (Nd:YAG) laser [66,67], with a working wavelength $\lambda = 1064$ nm, and an incident electric field amplitude $E_0 = 10^6$ V/m (intensity ~ 133 kW/cm²) [68]. The results are analogous to the ones observed in the GHz regime, including for slab1 and slab2. Because several techniques to develop these types of metamaterials are available, though the experimental realization may be challenging, we expect that the concepts presented here will stimulate exploitation of strong light-matter interactions in metamaterials to enhance SH conversion efficiency.

IV. CONCLUSIONS

In summary, we have shown that the defect mode in the bulk PP gap can be used to enhance SH conversion efficiency. In particular, we numerically demonstrated an enhancement of at least four orders of magnitude in SH conversion, for both the microwave and infrared regimes, which is controlled by increasing the angle of incidence. A giant enhancement can also be reached in one-dimensional PCs conveniently designed to satisfy the condition under which the SH wave coincides with the Bragg gap edge or with the defect mode.

ACKNOWLEDGMENTS

We acknowledge the financial support from the Colombian agency COLCIENCIAS and the Brazilian Agencies CNPq and FAPESP (2013/14262-7 and 2016/12311-9). This work is part of the project 1106-712-49884 (Contract No. 264-2016), supported by COLCIENCIAS (Fondo Nacional de Financiamiento para la Ciencia, la Tecnología y la Innovación, “Francisco José de Caldas”).

[1] J. B. Pendry, A. J. Holden, D. J. Robbins, and W. J. Stewart, *IEEE Trans. Microwave Theory Tech.* **47**, 2075 (1999).
 [2] D. R. Smith, W. J. Padilla, D. C. Vier, S. C. Nemat-Nasser, and S. Schultz, *Phys. Rev. Lett.* **84**, 4184 (2000).
 [3] R. A. Shelby, D. R. Smith, and S. Schultz, *Science* **292**, 77 (2001).

[4] A. Grbic and G. V. Eleftheriades, *J. Appl. Phys.* **92**, 5930 (2002).
 [5] G. V. Eleftheriades, A. K. Iyer, and P. C. Kremer, *IEEE Trans. Microwave Theory Tech.* **50**, 2702 (2002).
 [6] T. J. Yen, W. J. Padilla, N. Fang, D. C. Vier, D. R. Smith, J. B. Pendry, D. N. Basov, and X. Zhang, *Science* **303**, 1494 (2004).

- [7] S. Linden, C. Enkrich, M. Wegener, J. F. Zhou, T. Koschny, and C. M. Soukoulis, *Science* **306**, 1351 (2004).
- [8] S. Zhang, W. J. Fan, B. K. Minhas, A. Frauenglass, K. J. Malloy, and S. R. J. Brueck, *Phys. Rev. Lett.* **94**, 037402 (2005).
- [9] C. M. Soukoulis, S. Linden, and M. Wegener, *Science* **315**, 47 (2007).
- [10] H. J. Lezec, J. A. Dionne, and H. A. Atwater, *Science* **316**, 430 (2007).
- [11] W. Wu, E. Kim, E. Ponizovskaya, Y. Liu, Z. Yu, N. Fang, Y. R. Shen, A. M. Bratkovsky, W. Tong, C. Sun, X. Zhang, S.-Y. Wang, and R. S. Williams, *Appl. Phys. A* **87**, 143 (2007).
- [12] C. García-Meca, R. Ortuño, R. Salvador, A. Martínez, and J. Martí, *Opt. Exp.* **15**, 9320 (2007).
- [13] Q. Zhao, L. Kang, B. Du, H. Zhao, Q. Xie, X. Huang, B. Li, J. Zhou, and L. Li, *Phys. Rev. Lett.* **101**, 027402 (2008).
- [14] J. Valentine, S. Zhang, T. Zentgraf, E. Ulin-Avila, D. A. Genov, G. Bartal, and X. Zhang, *Nature (London)* **455**, 376 (2008).
- [15] Y. J. Jen, A. Lakhtakia, C. W. Yu, and C. T. Lin, *Opt. Express* **17**, 7784 (2009).
- [16] N. Limberopoulos, A. Akyurtlu, K. Higginson, A.-G. Kussow, and C. D. Merritt, *Appl. Phys. Lett.* **95**, 023306 (2009).
- [17] Y. J. Huang, G. J. Wen, T. Q. Li, and K. Xie, *J. Electromagn. Anal. Appl.* **2**, 104 (2010).
- [18] S. Xiao, V. P. Drachev, A. V. Kildishev, X. Ni, U. K. Chettiar, H.-J. Yuan, and V. M. Shalaev, *Nature (London)* **466**, 735 (2010).
- [19] C. García-Meca, J. Hurtado, J. Martí, A. Martínez, W. Dickson, and A. V. Zayats, *Phys. Rev. Lett.* **106**, 067402 (2011).
- [20] Y. Minowa, M. Nagai, H. Tao, K. Fan, A. C. Strikwerda, X. Zhang, R. D. Averitt, and K. Tanaka, *IEEE Trans. Terahertz Sci. Technol.* **1**, 441 (2011).
- [21] R. Paniagua-Domínguez, D. R. Abujetas, and J. A. Sánchez-Gil, *Sci. Rep.* **3**, 1507 (2013).
- [22] S. Zhou, S. Townsend, Y. M. Xie, X. Huang, J. Shen, and Q. Li, *Opt. Lett.* **39**, 2415 (2014).
- [23] B. Gong, X. Zhao, Z. Pan, S. Li, X. Wang, Y. Zhao, and C. Luo, *Sci. Rep.* **4**, 4713 (2014).
- [24] D. A. Lee, L. J. Vedral, D. A. Smith, R. L. Musselman, and A. O. Pinchuk, *AIP Adv.* **5**, 047119 (2015).
- [25] S. Lee, B. Kang, H. Keum, N. Ahmed, J. A. Rogers, P. M. Ferreira, S. Kim, and B. Min, *Sci. Rep.* **6**, 27621 (2016).
- [26] H. T. Nguyen, T. S. Bui, S. Yan, G. A. E. Vandenbosch, P. Lievens, L. D. Vu, and E. Janssens, *Appl. Phys. Lett.* **109**, 221902 (2016).
- [27] V. G. Veselago, *Sov. Phys. Usp.* **10**, 509 (1968).
- [28] J. Li, L. Zhou, C. T. Chan, and P. Sheng, *Phys. Rev. Lett.* **90**, 083901 (2003).
- [29] E. Reyes-Gómez, D. Mogilevtsev, S. B. Cavalcanti, C. A. A. de Carvalho, and L. E. Oliveira, *Europhys. Lett.* **88**, 24002 (2009).
- [30] H. Jiang, H. Chen, H. Li, Y. Zhang, and S. Zhu, *Appl. Phys. Lett.* **83**, 5386 (2003).
- [31] J. Li, D. Zhao, and Z. Liu, *Phys. Lett. A* **332**, 461 (2004).
- [32] U. Hempelmann, *IEEE J. Quantum Electron.* **35**, 1834 (1999).
- [33] X. Gan, X. Yao, R.-J. Shiue, F. Hatami, and D. Englund, *Opt. Express* **23**, 12998 (2015).
- [34] G. D'Aguanno, N. Mattiucci, M. Scalora, and M. J. Bloemer, *Laser Phys.* **15**, 590 (2005).
- [35] M. Tlidi, P. Kockaert, and L. Gelens, *Phys. Rev. A* **84**, 013807 (2011).
- [36] W. Chen and D. L. Mills, *Phys. Rev. Lett.* **58**, 160 (1987).
- [37] R. S. Hegde and H. G. Winful, *Opt. Lett.* **30**, 1852 (2005).
- [38] S. B. Cavalcanti, P. A. Brandão, A. Bruno-Alfonso, and L. E. Oliveira, *Opt. Lett.* **39**, 178 (2014).
- [39] N. Mattiucci, G. D'Aguanno, M. J. Bloemer, and M. Scalora, *Phys. Rev. E* **72**, 066612 (2005).
- [40] G. D'Aguanno, N. Mattiucci, M. Scalora, and M. J. Bloemer, *Phys. Rev. E* **74**, 026608 (2006).
- [41] G. D'Aguanno, N. Mattiucci, M. J. Bloemer, and M. Scalora, *Phys. Rev. E* **73**, 036603 (2006).
- [42] B.-Q. Chen, M.-L. Ren, R.-J. Liu, C. Zhang, Y. Sheng, B.-Q. Ma, and Z.-Y. Li, *Light: Sci. Appl.* **3**, e189 (2014).
- [43] C.-M. Lai, K.-H. Chang, Z.-Y. Yang, S.-H. Fu, S.-T. Tsai, C.-W. Hsu, N. E. Yu, A. Boudrioua, A. H. Kung, and L.-H. Peng, *Appl. Phys. Lett.* **105**, 221101 (2014).
- [44] Z. Lin, X. Liang, M. Lončar, S. G. Johnson, and A. W. Rodriguez, *Optica* **3**, 233 (2015).
- [45] M. S. Mohamed, A. Simbula, J.-F. Carlin, M. Minkov, D. Gerace, V. Savona, N. Grandjean, M. Galli, and R. Houdré, *APL Photonics* **2**, 031301 (2017).
- [46] B. Shi, Z. M. Jiang, and X. Wang, *Opt. Lett.* **26**, 1194 (2001).
- [47] F.-F. Ren, R. Li, C. Cheng, H.-T. Wang, J. Qiu, J. Si, and K. Hirao, *Phys. Rev. B* **70**, 245109 (2004).
- [48] Q. Zhu, D. Wang, and Y. Zhang, *J. Opt. A: Pure Appl. Opt.* **10**, 025201 (2008).
- [49] Q. G. Du, F.-F. Ren, C. H. Kam, and X. W. Sun, *Opt. Express* **17**, 6682 (2009).
- [50] T. S. Parvini, M. M. Tehranchi, and S. M. Hamidi, *Appl. Phys. A* **118**, 1447 (2015).
- [51] T. V. Dolgova, A. I. Maidikovski, M. G. Martemyanov, A. A. Fedyanin, O. A. Aktsipetrov, G. Marowsky, V. A. Yakovlev, G. Mattei, N. Ohta, and S. Nakabayashi, *J. Opt. Soc. Am. B* **19**, 2129 (2002).
- [52] P. Simesen, T. Søndergaard, E. Skovsen, J. Fiutowski, H.-G. Rubahn, S. I. Bozhevolnyi, and K. Pedersen, *Opt. Express* **23**, 16356 (2015).
- [53] A. de Hoogh, A. Opheij, M. Wulf, N. Rotenberg, and L. Kuipers, *ACS Photonics* **3**, 1446 (2016).
- [54] H. C. Zhang, Y. Fan, J. Guo, X. Fu, and T. J. Cui, *ACS Photonics* **3**, 139 (2016).
- [55] M. E. Inchaussandague, M. L. Gigli, K. A. O'donnell, E. R. Méndez, R. Torre, and C. I. Valencia, *J. Opt. Soc. Am. B* **34**, 27 (2017).
- [56] F. Reyes Gómez and J. R. Mejía-Salazar, *Opt. Lett.* **40**, 5034 (2015).
- [57] Y. Chen, *Appl. Phys. Lett.* **92**, 011925 (2008).
- [58] Y. Chen, *J. Opt. Soc. Am. B* **25**, 1794 (2008).
- [59] Y. Chen, *J. Phys. D: Appl. Phys.* **42**, 075106 (2009).
- [60] N. Ouchani, D. Bria, B. Djafari-Rouhani, and A. Nougaoui, *J. Appl. Phys.* **106**, 113107 (2009).
- [61] Z. Lu, *Opt. Lett.* **36**, 573 (2011).
- [62] H. Li, J. W. Haus, and P. Banerjee, *J. Opt. Soc. Am. B* **32**, 1456 (2015).
- [63] G. D. Boyd, T. J. Bridges, M. A. Pollack, and E. H. Turner, *Phys. Rev. Lett.* **26**, 387 (1971).

- [64] *Infrared and Millimeter Waves*, edited by K. J. Button (Academic, New York, 1983), Vol. 9, Part I, Chap. 3C.
- [65] K. Busch, C. T. Chan, and C. M. Soukoulis, in *Photonic Band Gap Materials*, edited by C. M. Soukoulis (Kluwer, Dordrecht, 1996).
- [66] S. T. Yang, C. C. Pohalski, E. K. Gustafson, R. L. Byer, R. S. Feigelson, R. J. Raymakers, and R. K. Route, *Opt. Lett.* **16**, 1493 (1991).
- [67] A. Suzuki, T. Matsushita, T. Aoki, Y. Yoneyama, and M. Okuda, *Jpn. J. Appl. Phys.* **38**, L71 (1999).
- [68] M.-L. Ren and Z.-Y. Li, *Appl. Phys. A* **107**, 71 (2012).